*International Journal of Thermophysics, Vol. 24, No. 5, September 2003 (© 2003)*

# Viscosity and Liquid Density of Asymmetric Hydrocarbon Mixtures[1]

**A. J. Queimada,[2,3] S. E. Quiñones-Cisneros,[2] I. M. Marrucho,[3] J. A. P. Coutinho,[3] and E. H. Stenby[2,4]**

Although a large body of viscosity data exists for simple mixtures of lighter *n*-alkanes, available information for heavy or asymmetric systems is scarce. Experimental measurements of viscosity and liquid densities were performed, at atmospheric pressure, in pure and mixed *n*-heptane, *n*-hexadecane, *n*-eicosane, *n*-docosane, and *n*-tetracosane from 293.15 K, or above the melting point, up to 343.15 K. The measured densities were correlated using the Peng–Robinson equation of state, and viscosities were modelled using the friction theory.

**KEY WORDS:** friction theory; liquid density; mixtures; *n*-alkanes; *n*-docosane; *n*-eicosane; *n*-heptane; *n*-hexadecane; *n*-tetracosane; paraffins; Peng–Robinson EOS; viscosity.

## 1. INTRODUCTION

Due to the continuous development of the chemical industry, it is becoming quite common to find systems in which considerable differences in size exists between the heavier and lighter components of a mixture. In oil extraction and handling processes, the importance of asymmetric systems is emerging. As a result of the increasing depletion of oil reservoirs, the interest in the heavier oil fractions has grown considerably. Several engineering developments were adopted which allowed increases in the oil extraction yields. This increase was accomplished by the extraction of

[1] Paper presented at the Sixteenth European Conference on Thermophysical Properties, September 1–4, 2002, London, United Kingdom.

[2] Engineering Research Center IVC-SEP, Department of Chemical Engineering, Technical University of Denmark, Building 229, DK-2800 Kgs. Lyngby, Denmark.

[3] CICECO, Chemistry Department, Aveiro University, 3810-193 Aveiro, Portugal.

[4] To whom correspondence should be addressed. E-mail: ehs@kt.dtu.dk



0195-928X/03/0900-1221/0 © 2003 Plenum Publishing Corporation

heavier components which were not extracted before, making components of the new oils more asymmetric. To develop the extraction and handling processes of these heavy oils, several thermophysical properties in a broad range of conditions should be available. Two valuable properties to model oil extraction from reservoirs are viscosity and liquid density.

The importance of viscosity is well known. All equations expressing the flow of fluids contain this property, and several product characteristics can be largely determined by its magnitude. Lubricants and paints are also examples of products for which the viscosity is one of the key properties and where asymmetric systems are important.

Generally, it is much easier to find open literature studies of phase equilibria rather than studies on non-equilibrium properties such as viscosity. Although literature data have been substantially increased over the last few decades, information about asymmetric or heavy systems is still scarce.

This work is part of a broader project that involves measurements and modelling of viscosity, liquid density, and surface tension of several mixtures of a paraffin (*n*-eicosane (*n*-$C_{20}H_{42}$), *n*-docosane (*n*-$C_{22}H_{46}$), and *n*-tetracosane (*n*-$C_{24}H_{50}$) with a smaller *n*-alkane (*n*-heptane (*n*-$C_7H_{16}$), *n*-decane ($C_{10}H_{22}$), or *n*-hexadecane (*n*-$C_{16}H_{34}$)).

In this paper, the viscosity and corresponding liquid density measurements and modelling of four binary and one ternary mixtures are reported: *n*-heptane + *n*-eicosane, *n*-heptane + *n*-docosane, *n*-heptane + *n*-tetracosane, *n*-hexadecane + *n*-eicosane, and *n*-heptane + *n*-eicosane + *n*-tetracosane.

## 2. EXPERIMENTAL

The following chemicals were used in the measurements: *n*-heptane (Rathburn, $\geqslant 99$ wt.%), *n*-hexadecane (Aldrich, $\geqslant 99$ wt.%), *n*-eicosane (Aldrich, $\geqslant 99$ wt.%), *n*-docosane (Aldrich, $\geqslant 99$ wt.%), and *n*-tetracosane (Aldrich, $\geqslant 99$ wt%). No further purification was carried out.

A rolling ball microviscometer from Anton PAAR KG (AMV 200 Automated Microviscometer) was used. This apparatus is based on the measurement of the time that a steel ball needs to roll down inside a glass capillary filled with sample. Several combinations of ball/capillary of different diameters can be selected, giving the possibility of measuring viscosities from 0.5 to 800 mPa·s. One of the advantages of this technique is that it requires very small amounts of sample. Depending on the capillary, only 0.12 to 2.5 $cm^3$ are used. The measurement is fully automatic. Two magnetic sensors are used to determine the rolling time which is reported within $\pm 0.01$ s. Shear stress can be varied by selecting different rolling angles, and up to ten different rolling angles (both positive and negative) can be chosen from 15 to 90°. Up to six repetitions can be programmed for each angle.

The temperature was controlled in the viscometer by the use of a Heto thermostatic circulator. The temperature was measured by a built-in temperature sensor, placed closed to the capillary surface, enclosed in a thermostatic capillary block on whose walls the thermostatic water circulates. The temperature working range for this instrument is 279.15 to 353.15 K with an uncertainty of $\pm 0.01$ K.

The viscosity is calculated from the rolling times and the liquid density using the following equation:

$$\eta = \kappa(\alpha)\, t(\rho_{\text{ball}} - \rho_{\text{liquid}}) \tag{1}$$

where $\eta$ is the viscosity (mPa·s), $\kappa$ is a calibration constant which only depends on the angle $\alpha$, $t$ is the roll time (s), and $\rho$ is the density ($\text{kg}\cdot\text{m}^{-3}$).

The parameter $\kappa$ has to be determined, for each angle $\alpha$, with liquids of known viscosity and density. In this work, distilled water, and Cannon Instruments Co. and HAAKE Medingen Gmbh viscosity standards were used for calibration. These standards were selected to cover the entire measuring range.

The liquid density was determined in an Anton PAAR DMA 58 unit, which is based on the vibrating U-tube method. It is used to measure oscillating periods that are automatically converted to liquid densities after calibration. Two density standards have to be selected for calibration, at each temperature. In this work, air and distilled water were used as calibrating fluids. This instrument can operate from 263.15 to 343.15 K, and it uses approximately 0.7 $\text{cm}^3$ of sample. The temperature is kept constant with a built-in Peltier element that can control temperature in the cell within $\pm 0.005$ K. The temperature is determined with an uncertainty of $\pm 0.01$ K and density values within $\pm 10^{-2}\ \text{kg}\cdot\text{m}^{-3}$.

Mixtures were carefully prepared by weighing the components on a Sartorius analytical balance ($\pm 0.0001$ g). After preparation, solutions were kept in the refrigerator between measurements.

Following the measurements, the viscometer capillary and the densimeter cell were carefully cleaned with toluene and ethanol. In the end they were dried with vacuum and compressed air, respectively.

## 3. MODELING

The *friction theory*, recently proposed by Quiñones-Cisneros et al. [1–5] was used for the viscosity modelling. This general model has been applied successfully for viscosity predictions of several different mixtures, such as those involving hydrocarbons [1, 2], crude oil systems [3], light

gases [4], and carbon dioxide + hydrocarbon mixtures [5] over a broad temperature and pressure range.

In this work, the simplest form of the *friction theory* (or *f-theory*) as described in Quiñones-Cisneros et al. [2] was used. The viscosity is modelled from a mechanical viewpoint, separating it into two contributions, one arising from the dilute gas and the other from the friction between layers:

$$\eta = \eta_0 + \eta_f \tag{2}$$

where $\eta$ represents the viscosity, in mPa·s, and the subscripts 0 and f stand for dilute gas and friction, respectively.

The dilute gas viscosity is calculated as a function of temperature $T$ (K), from the Chung et al. model [6] using the critical volume $v_c$ ($m^3 \cdot mol^{-1}$), the critical temperature $T_c$ (K), the molecular weight $MW$ ($kg \cdot mol^{-1}$), and the acentric factor $\omega$:

$$\eta_0 = 0.12897 \frac{\sqrt{MWT}}{v_c^{2/3}\Omega^*} F_c \tag{3}$$

$$\Omega^* = \frac{1.16145}{T^{*0.14874}} + \frac{0.52487}{\exp(0.77320T^*)} + \frac{2.16178}{\exp(2.43787T^*)} - 6.435 \times 10^{-4} T^{*0.14874} \sin(18.0323T^{*-0.76830} - 7.27371) \tag{4}$$

$$T^* = \frac{1.2593T}{T_c} \tag{5}$$

$$F_c = 1 - 0.2756\omega \tag{6}$$

An additional term, originally present in Eq. (6) accounting for hydrogen bonding and polarity, was dropped due to the nonpolar nature of the systems reported in this work.

In Eq. (2), the friction contribution is related to a van der Waals type of equation-of-state repulsive and attractive pressures by means of temperature-dependent friction coefficients, $\hat{\kappa}$.

$$\eta_f = \left[ \hat{\kappa}_r \times \frac{p_r}{p_c} + \hat{\kappa}_{rr} \times \left( \frac{p_r}{p_c} \right)^2 + \hat{\kappa}_a \times \frac{p_a}{p_c} \right] \times \eta_c \tag{7}$$

where $p$ stands for the pressure (Pa), both subscripts r and rr represent repulsive, and c and a represent critical and attractive, respectively. $\eta_c$ is a pure component characteristic critical viscosity.

The friction coefficients depend only on the equation-of-state used to obtain the attractive and repulsive pressures, $p_a$ and $p_c$. In this work, the Peng–Robinson (PR) [7] equation of state was combined with the PR f-theory one-parameter general model [2].

For the characteristic critical viscosity the following equation was used [2]:

$$\eta_c = 3.8136 \times 10^{-8} p_c MW^{0.601652} \tag{8}$$

The extension to mixtures follows from the properties of the pure components:

$$\eta_{mx} = \eta_{0_{mx}} + \eta_{f_{mx}} \tag{9}$$

$$\eta_{0_{mx}} = \exp\left[\sum_{i=1}^{n} x_i \ln(\eta_{0_i})\right] \tag{10}$$

$$\eta_{f_{mx}} = \kappa_{r_{mx}} p_r + \kappa_{rr_{mx}} p_r^2 + \kappa_{a_{mx}} p_a \tag{11}$$

$$\kappa_{r_{mx}} = \sum_{i=1}^{n} z_i \frac{\eta_{c_i} \hat{\kappa}_{r_i}}{p_{c_i}} \tag{12}$$

$$\kappa_{rr_{mx}} = \sum_{i=1}^{n} z_i \frac{\eta_{c_i} \hat{\kappa}_{rr_i}}{p_{c_i}^2} \tag{13}$$

$$\kappa_{a_{mx}} = \sum_{i=1}^{n} z_i \frac{\eta_{c_i} \hat{\kappa}_{a_i}}{p_{c_i}} \tag{14}$$

$$z_i = \frac{x_i}{MW_i^{0.3} \sum_{i=1}^{n} \frac{x_i}{MW_i^{0.3}}} \tag{15}$$

where mx represents a mixture property, $n$ is the number of components, and $x_i$ is the mole fraction of the $i$th component.

## 4. RESULTS AND DISCUSSION

Both viscosity and liquid density were measured, at atmospheric pressure, from 293.15 K (or above the melting point) up to 343.15 K in temperature intervals of 10 K. In Tables I to V the measured viscosities are reported. Each viscosity measurement was performed at 10 different rolling angles from 15.0 to 46.5° with four repetitions at each value. Each reported data point is thus an average of 40 different viscosity measurements.

The corresponding liquid densities are reported in Tables VI to X. It should be noted that, for *n*-heptane, although liquid density data are

**Table I.** Viscosity (mPa·s) of the Binary Mixture *n*-Heptane + *n*-Eicosane

| $xC_{20}H_{42}$ | 293.2 K | 303.2 K | 313.2 K | 323.2 K | 333.1 K | 343.1 K |
|---|---|---|---|---|---|---|
| 0.000 | 0.4084 | 0.3725 | 0.3447 | 0.3182 | | |
| 0.200 | 0.9382 | 0.8194 | 0.7187 | 0.6384 | 0.5737 | 0.5184 |
| 0.400 | | 1.567 | 1.327 | 1.142 | 0.9891 | 0.8693 |
| 0.499 | | 2.020 | 1.705 | 1.452 | 1.259 | 1.107 |
| 0.597 | | | 2.145 | 1.812 | 1.539 | 1.337 |
| 0.796 | | | 2.989 | 2.456 | 2.058 | 1.760 |
| 1.000 | | | 4.010 | 3.195 | 2.611 | 2.171 |

**Table II.** Viscosity (mPa·s) of the Binary Mixture *n*-Heptane + *n*-Docosane

| $xC_{22}H_{46}$ | 303.2 K | 313.2 K | 323.1 K | 333.1 K | 343.2 K |
|---|---|---|---|---|---|
| 0.000 | 0.3725 | 0.3447 | 0.3182 | | |
| 0.200 | 0.9761 | 0.8502 | 0.7493 | 0.6682 | 0.6010 |
| 0.400 | | 1.621 | 1.390 | 1.231 | 1.100 |
| 0.479 | | 2.137 | 1.826 | 1.549 | 1.332 |
| 0.596 | | | 2.449 | 2.041 | 1.734 |
| 0.798 | | | 3.197 | 2.648 | 2.245 |
| 1.000 | | | 4.128 | 3.342 | 2.754 |

**Table III.** Viscosity (mPa·s) of the Binary Mixture *n*-Heptane + *n*-Tetracosane

| $xC_{24}H_{50}$ | 313.2 K | 323.2 K | 333.1 K | 343.2 K |
|---|---|---|---|---|
| 0.000 | 0.3447 | 0.3182 | | |
| 0.198 | 0.9672 | 0.8535 | 0.7619 | 0.6775 |
| 0.398 | | 1.675 | 1.443 | 1.262 |
| 0.497 | | 2.241 | 1.895 | 1.631 |
| 0.596 | | 2.599 | 2.200 | 1.862 |
| 0.796 | | | 3.289 | 2.628 |
| 1.000 | | | 4.477 | 3.666 |

**Table IV.** Viscosity (mPa·s) of the Binary Mixture *n*-Hexadecane + *n*-Eicosane

| $xC_{20}H_{42}$ | 293.2 K | 303.2 K | 313.2 K | 323.2 K | 333.2 K | 343.2 K |
|---|---|---|---|---|---|---|
| 0.000 | 3.507 | 2.780 | 2.264 | 1.879 | 1.590 | 1.366 |
| 0.200 | 3.875 | 3.045 | 2.459 | 2.028 | 1.709 | 1.469 |
| 0.400 | | 3.481 | 2.785 | 2.295 | 1.907 | 1.622 |
| 0.500 | | 3.770 | 3.011 | 2.464 | 2.036 | 1.717 |
| 0.599 | | 4.065 | 3.223 | 2.621 | 2.188 | 1.837 |
| 0.800 | | | 3.602 | 2.918 | 2.416 | 2.032 |
| 1.000 | | | 4.010 | 3.195 | 2.611 | 2.171 |

**Table V.** Viscosity (mPa·s) of the Ternary System *n*-Heptane + *n*-Eicosane + *n*-Tetracosane

| $xC_{20}H_{42}$ | $xC_{24}H_{50}$ | 303.2 K | 313.2 K | 323.1 K | 333.2 K | 343.1 K |
|---|---|---|---|---|---|---|
| 0.000 | 0.000 | 0.3725 | 0.3447 | 0.3182 | | |
| 0.100 | 0.100 | 0.9397 | 0.8123 | 0.7162 | 0.6517 | 0.5836 |
| 0.200 | 0.200 | | 1.655 | 1.418 | 1.231 | 1.073 |
| 0.249 | 0.249 | | 2.248 | 1.912 | 1.636 | 1.410 |
| 0.300 | 0.300 | | 2.737 | 2.271 | 1.932 | 1.638 |
| 0.399 | 0.399 | | | 3.049 | 2.547 | 2.146 |
| 0.500 | 0.500 | | | 4.134 | 3.334 | 2.750 |

**Table VI.** Liquid Density ($kg \cdot m^{-3}$) of the Binary Mixture *n*-Heptane + *n*-Eicosane

| $xC_{20}H_{42}$ | 293.15 K | 303.15 K | 313.15 K | 323.15 K | 333.15 K | 343.13 K |
|---|---|---|---|---|---|---|
| 0.000 | 683.59 | 675.35 | 666.74 | 657.97 | 649.11 | 640.16 |
| 0.200 | 724.94 | 717.44 | 709.73 | 701.91 | 694.09 | 686.30 |
| 0.400 | | 742.70 | 735.49 | 728.35 | 721.13 | 713.92 |
| 0.498 | | 752.39 | 745.65 | 738.70 | 731.65 | 724.75 |
| 0.597 | | | 755.55 | 748.85 | 741.84 | 735.36 |
| 0.796 | | | 765.22 | 758.65 | 751.95 | 745.29 |
| 1.000 | | | 775.13 | 768.33 | 761.72 | 755.07 |

**Table VII.** Liquid Density ($kg \cdot m^{-3}$) of the Binary Mixture *n*-Heptane + *n*-Docosane

| $xC_{22}H_{46}$ | 303.15 K | 313.15 K | 323.15 K | 333.15 K | 343.13 K |
|---|---|---|---|---|---|
| 0.000 | 675.35 | 666.74 | 657.97 | 649.11 | 640.16 |
| 0.200 | 722.13 | 713.83 | 706.92 | 699.53 | 691.82 |
| 0.400 | | 741.03 | 734.90 | 727.95 | 720.67 |
| 0.479 | | 749.62 | 743.30 | 736.42 | 729.69 |
| 0.596 | | | 753.11 | 746.47 | 739.81 |
| 0.798 | | | 764.79 | 758.12 | 751.66 |
| 1.000 | | | 774.25 | 767.67 | 761.12 |

**Table VIII.** Liquid Density ($kg \cdot m^{-3}$) of the Binary Mixture *n*-Heptane + *n*-Tetracosane

| $xC_{24}H_{50}$ | 313.15 K | 323.15 K | 333.15 K | 343.13 K |
|---|---|---|---|---|
| 0.000 | 666.74 | 657.97 | 649.11 | 640.16 |
| 0.198 | 718.81 | 711.25 | 703.69 | 696.16 |
| 0.398 | | 740.90 | 734.09 | 726.89 |
| 0.498 | | 752.08 | 745.74 | 739.08 |
| 0.595 | | 757.72 | 750.93 | 744.17 |
| 0.796 | | | 763.75 | 757.20 |
| 1.000 | | | 772.72 | 766.24 |

**Table IX.** Liquid Density ($kg \cdot m^{-3}$) of the Binary Mixture *n*-Hexadecane + *n*-Eicosane

| $xC_{20}H_{42}$ | 293.15 K | 303.15 K | 313.15 K | 323.15 K | 333.15 K | 343.13 K |
|---|---|---|---|---|---|---|
| 0.000 | 773.33 | 766.40 | 759.48 | 752.58 | 745.62 | 738.80 |
| 0.200 | 776.80 | 769.93 | 763.12 | 756.18 | 749.33 | 742.50 |
| 0.400 | | 773.33 | 766.20 | 759.69 | 752.88 | 746.12 |
| 0.500 | | 774.66 | 768.03 | 761.14 | 754.37 | 747.64 |
| 0.599 | | 776.21 | 769.54 | 762.66 | 755.89 | 749.17 |
| 0.800 | | | 772.61 | 765.84 | 759.16 | 752.38 |
| 1.000 | | | 775.13 | 768.33 | 761.72 | 755.07 |

**Table X.** Liquid Density ($kg \cdot m^{-3}$) of the Ternary Mixture *n*-Heptane + *n*-Eicosane + *n*-Tetracosane

| $xC_{20}H_{42}$ | $xC_{24}H_{50}$ | 303.15 K | 313.15 K | 323.15 K | 333.15 K | 343.13 K |
|---|---|---|---|---|---|---|
| 0.000 | 0.000 | 675.35 | 666.74 | 657.97 | 649.11 | 640.16 |
| 0.100 | 0.100 | 719.28 | 714.64 | 706.87 | 699.24 | 691.51 |
| 0.200 | 0.200 | | 741.76 | 733.78 | 727.13 | 720.62 |
| 0.249 | 0.249 | | 751.10 | 744.08 | 737.24 | 730.33 |
| 0.300 | 0.300 | | 759.26 | 752.22 | 745.16 | 738.30 |
| 0.397 | 0.397 | | | 764.52 | 757.68 | 751.09 |
| 0.500 | 0.500 | | | 774.31 | 767.69 | 760.43 |

reported over the full temperature range, the viscosity is only reported up to 323.2 K, since at the highest temperatures, considerable deviations were found with literature data. These measurements would also correspond to a measuring range substantially below the lower limit suggested by the viscometer manufacturer.

In Table XI a comparison of the measured densities and viscosities with literature pure component data [8–19] is presented. No data were found for any of the mixtures. Very low average absolute deviations, below 0.1%, were found for the liquid densities. Viscosity deviations are somewhat higher, but still below 5% with the maximum deviation found for *n*-tetracosane, for which only a small amount of experimental information is available. For the other *n*-alkanes the deviations are below 2%, and the average of all deviations is 1.9%, quite close to the values found by Dandekar et al. [20] for the same equipment.

With the information presented in Tables II, V, VII, and X, one can compare the results between the ternary $n\text{-}C_7H_{16} + n\text{-}C_{20}H_{42} + n\text{-}C_{24}H_{50}$ and the corresponding binary (in terms of the average chain length of the heavier components), $n\text{-}C_7H_{16} + n\text{-}C_{22}H_{46}$. Although the liquid densities are quite similar, the viscosity of the binary mixture $n\text{-}C_7H_{16} + n\text{-}C_{22}H_{46}$ is somewhat higher than that found for the equivalent ternary system. Similar conclusions from experimental studies of binary and quaternary *n*-alkane mixtures were reported by Wakefield et al. [19]. Recent studies using corresponding states theory [21] showed that, for pure components, the viscosity is not linear with the chain length. This topic shall be further studied in the future.

Modelling results are reported in Table XII and on Figs. 1–10. The *f-theory* was coupled with the Peng–Robinson equation of state (PR EOS). Preliminary results, showed that this equation of state is unable to produce accurate predictions of the liquid densities of heavy *n*-alkanes, with errors propagating to the viscosities, leading to poor viscosity results. Following

**Table XI.** Comparison of Measured Data with Literature

| | | Viscosity (mPa · s) | | | | | | | | | | | |
|---|---|---|---|---|---|---|---|---|---|---|---|---|---|
| *n*-alkane | *T* (K) | Exp. | DIPPR [8][1] | Wakefield et al. [19][2] | Vargaftik [14] | Ducoulombier et al. [13] | Giller et al. [11] | Knapstad et al. [12] | Doolittle et al. [9] | Assael et al. [15] | Aminhabavi et al. [16] | Aralaguppi et al. [17] | AAD (%)[3] |
| $n$-$C_7H_{16}$ | 293.2 | 0.4084 | 0.413 | | 0.4140 | 0.4145 | 0.410 | 0.4101 | 0.4180 | | | | 1.7 |
| | 303.2 | 0.3725 | 0.373 | | 0.3730 | 0.3740 | | | | 0.3675 | 0.368 | 0.372 | |
| | 313.2 | 0.3447 | 0.337 | | 0.3380 | 0.3380 | | | | | | | |
| | 323.2 | 0.3182 | 0.309 | | 0.3080 | 0.3080 | | | 0.3100 | 0.3041 | | | |
| $n$-$C_{16}H_{34}$ | 293.2 | 3.507 | 3.37 | | 3.451 | | | | | | | | 1.6 |
| | 303.2 | 2.780 | 2.74 | | 2.754 | | | | | | | | |
| | 313.2 | 2.264 | 2.24 | | 2.232 | 2.23 | | | | | | | |
| | 323.2 | 1.879 | 1.86 | | 1.852 | | | | | | | | |
| | 333.2 | 1.590 | 1.57 | | 1.560 | | | | | | | | |
| | 343.2 | 1.366 | 1.35 | | 1.338 | | | | | | | | |
| $n$-$C_{20}H_{42}$ | 313.2 | 4.010 | 4.06 | | 4.072 | | | | | | | | 2.0 |
| | 323.2 | 3.195 | 3.26 | | 3.259 | | | | | | | | |
| | 333.2 | 2.611 | 2.68 | | 2.665 | | | | | | | | |
| | 343.2 | 2.171 | 2.23 | | 2.220 | | | | | | | | |
| $n$-$C_{24}H_{50}$ | 333.2 | 4.477 | 4.23 | 4.32 | | | | | | | | | 4.7 |
| | 343.2 | 3.666 | | | | | | | | | | | |
| AAD (%)[3] | | | 2.1 | 3.6 | 1.7 | 1.7 | 0.39 | 0.41 | 2.5 | 3.0 | 1.2 | 0.13 | |

| *n*-alkane | $T$ (K) | Liquid density ($kg \cdot m^3$) Exp. | DIPPR [8][1] | Dutour et al. [10] | Doolittle et al. [9] | AAD (%)[3] |
|---|---|---|---|---|---|---|
| $n$-$C_7H_{16}$ | 293.15 | 683.59 | 683.76 | | | 0.02 |
| | 303.15 | 675.35 | 675.26 | | | |
| | 313.15 | 666.74 | 666.73 | | | |
| | 323.15 | 657.97 | 658.00 | | 658.2 | |
| | 333.15 | 649.11 | 648.90 | | | |
| | 343.13 | 640.16 | 639.91 | | | |
| $n$-$C_{16}H_{34}$ | 293.15 | 773.33 | 773.55 | | | 0.03 |
| | 303.15 | 766.40 | 766.44 | | | |
| | 313.15 | 759.48 | 759.51 | | | |
| | 323.15 | 752.58 | 752.81 | | | |
| | 333.15 | 745.62 | 746.11 | | | |
| | 343.13 | 738.80 | 739.31 | | | |
| $n$-$C_{20}H_{42}$ | 313.15 | 775.13 | 775.89 | | | 0.1 |
| | 323.15 | 768.33 | 769.17 | | | |
| | 333.15 | 761.72 | 762.49 | | | |
| | 343.13 | 755.07 | 755.98 | | | |
| $n$-$C_{22}H_{46}$ | 323.15 | 774.25 | 774.63 | | | 0.1 |
| | 333.15 | 767.67 | 768.45 | | | |
| | 343.13 | 761.12 | 762.24 | | | |
| $n$-$C_{24}H_{50}$ | 333.15 | 772.72 | 772.81 | 773.77 | | 0.05 |
| | 343.13 | 766.24 | 766.25 | 766.66 | | |
| AAD (%) [3] | | | 0.05 | 0.1 | 0.03 | |

[1] Average of reported experimental values.

[2] Interpolation of reported values at 328.16 and 338.16 K.

[3] AAD (%) $= \frac{100}{n} \sum_n \frac{|x_{\text{measured}} - x_{\text{exp}}|}{x_{\text{exp}}}$.

**Table XII.** Modeling Results Using Pure Component Properties Reported in Table XIII

| Mixture | Average absolute deviation (AAD) (%) | |
|---|---|---|
| | f-theory | PR EOS |
| $n$-$C_7H_{16}$–$n$-$C_{20}H_{42}$ | 7.1 | 0.8 |
| $n$-$C_7H_{16}$–$n$-$C_{22}H_{46}$ | 7.5 | 0.6 |
| $n$-$C_7H_{16}$–$n$-$C_{24}H_{50}$ | 8.0 | 0.7 |
| $n$-$C_{16}H_{34}$–$n$-$C_{20}H_{42}$ | 2.0 | 0.6 |
| $n$-$C_7H_{16}$–$n$-$C_{20}H_{42}$–$n$-$C_{24}H_{50}$ | 9.1 | 0.7 |
| Average (all data points) | 6.3 | 0.7 |

**Table XIII.** Pure Component Properties Used for Modeling

| $n$-alkane | $T_c$ (K) | $P_c$ (Pa × $10^{-5}$) | $V_c$ ($m^3 \cdot mol^{-1} \times 10^3$) | $\omega$ | $MW$ ($kg \cdot mol^{-1} \times 10^3$) |
|---|---|---|---|---|---|
| $n$-$C_7H_{16}$ | 540.20 | 27.40 | 0.42800 | 0.350 | 100.204 |
| $n$-$C_{16}H_{34}$ | 736.44 | 17.18 | 0.83516 | 0.718 | 226.446 |
| $n$-$C_{20}H_{42}$ | 751.14 | 14.10 | 0.99043 | 0.865 | 282.554 |
| $n$-$C_{22}H_{46}$ | 763.76 | 13.07 | 1.0624 | 0.963 | 310.607 |
| $n$-$C_{24}H_{50}$ | 783.98 | 12.29 | 1.1334 | 1.032 | 338.661 |

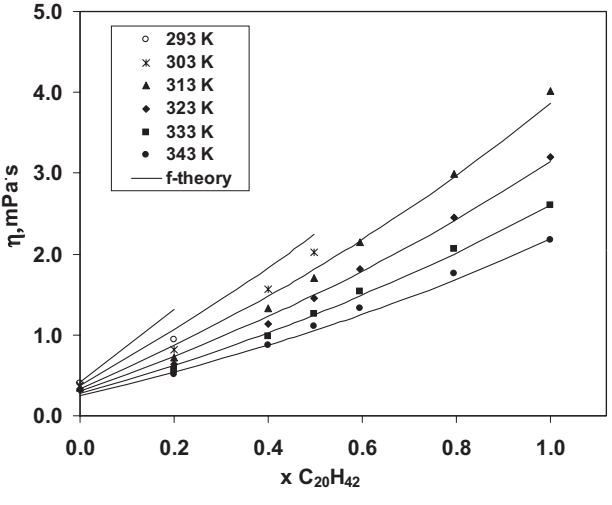


**Fig. 1.** Viscosity of the binary mixture $n$-$C_7H_{16} + n$-$C_{20}H_{42}$; experimental results and model predictions.

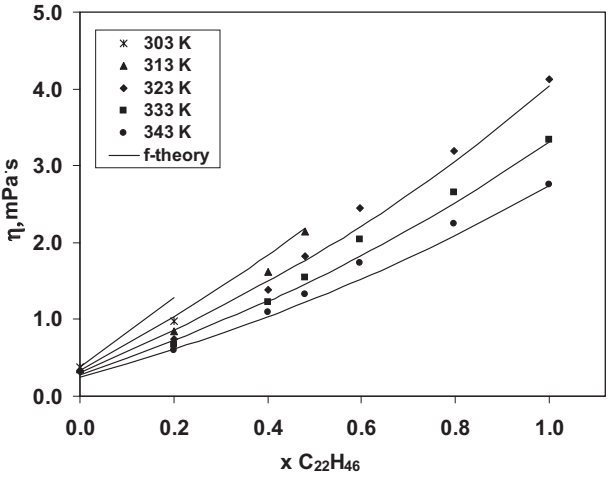


**Fig. 2.** Viscosity of the binary mixture $n$-$C_7H_{16} + n$-$C_{22}H_{46}$; experimental results and model predictions.

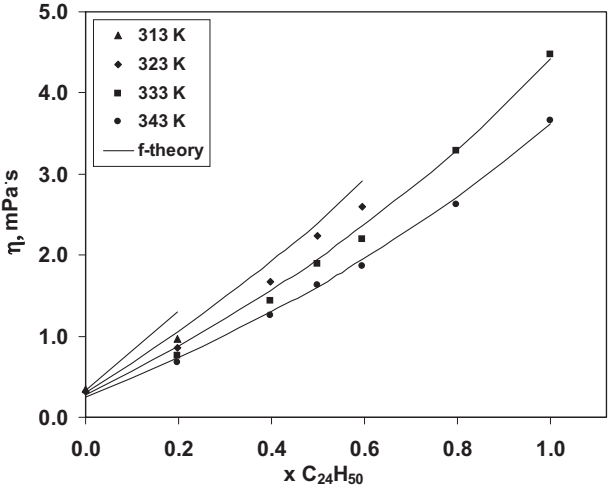


**Fig. 3.** Viscosity of the binary mixture $n$-$C_7H_{16} + n$-$C_{24}H_{50}$; experimental results and model predictions.

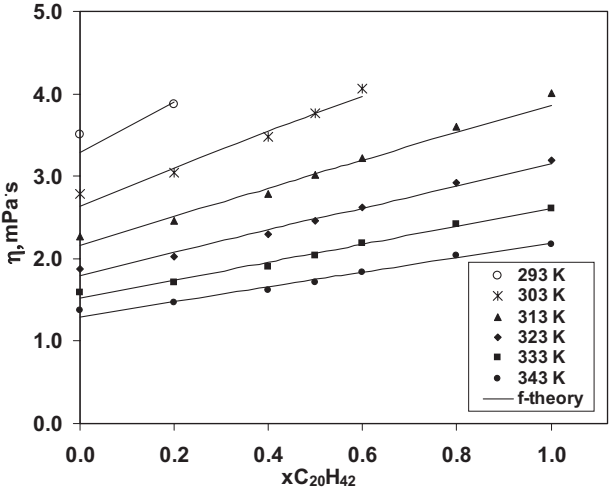


**Fig. 4.** Viscosity of the binary mixture $n$-$C_{16}H_{34} + n$-$C_{20}H_{42}$; experimental results and model predictions.

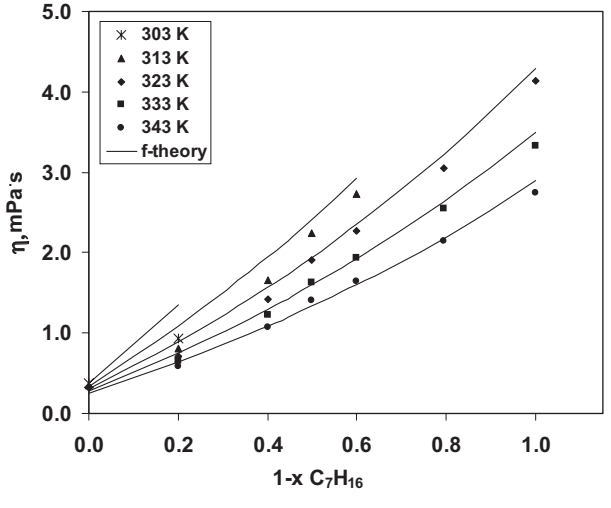


**Fig. 5.** Viscosity of the ternary mixture $n$-$C_7H_{16} + n$-$C_{20}H_{42} + n$-$C_{24}H_{50}$; experimental results and model predictions.

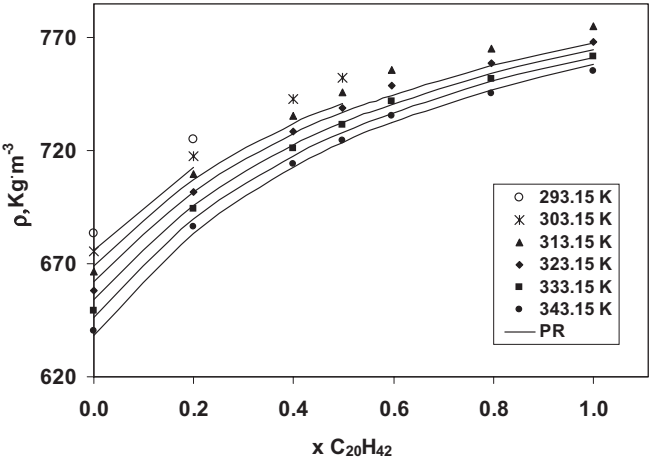


**Fig. 6.** Liquid density of the binary mixture $n$-$C_7H_{16} + n$-$C_{20}H_{42}$; experimental results and model predictions.

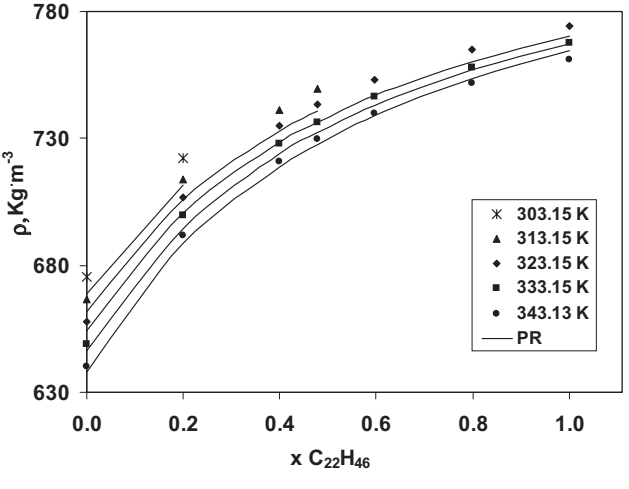


**Fig. 7.** Liquid density of the binary mixture $n$-$C_7H_{16} + n$-$C_{22}H_{46}$; experimental results and model predictions.

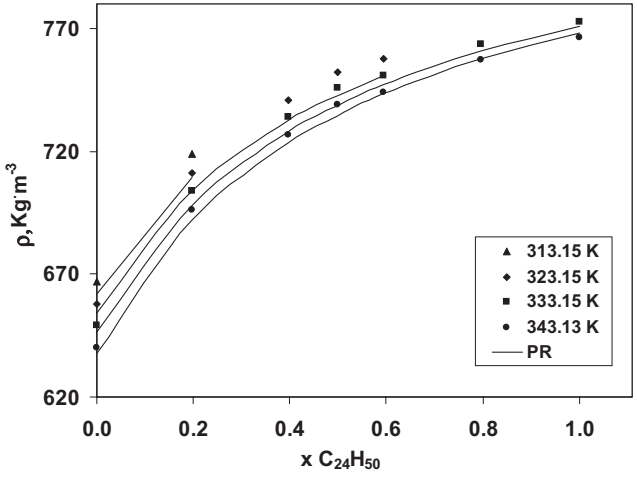


**Fig. 8.** Liquid density of the binary mixture $n$-$C_7H_{16} + n$-$C_{24}H_{50}$; experimental results and model predictions.

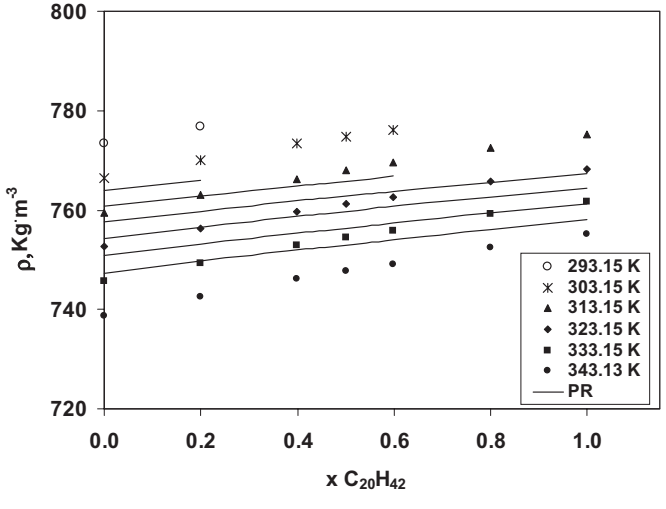


**Fig. 9.** Liquid density of the binary mixture $n$-$C_{16}H_{34} + n$-$C_{20}H_{42}$; experimental results and model predictions.

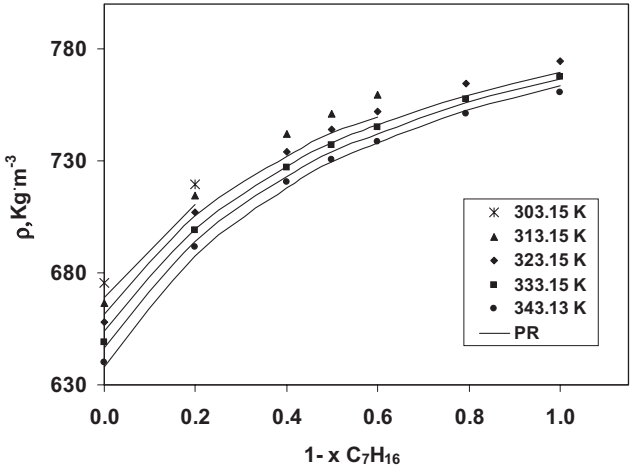


**Fig. 10.** Liquid density of the ternary mixture $n$-$C_7H_{16}$ + $n$-$C_{20}H_{42}$ + $n$-$C_{24}H_{50}$; experimental results and model predictions.

the approach used before with the friction theory, the critical properties of the heavy $n$-alkanes were fitted to the liquid densities. The fitted critical properties are reported in Table XIII. In Figs. 6–10 it is shown how the Peng–Robinson EOS with the new critical parameters can adequately represent the liquid density of the mixtures.

Generally, good viscosity predictions are obtained with the friction theory. Larger errors are obtained for the mixtures containing $n$-heptane, since these systems are the most asymmetric and no mixture information was used in either the EOS or in the f-theory. The heavier, but less asymmetric mixture, $n$-$C_{16}H_{34}$ + $n$-$C_{20}H_{42}$ shows that this viscosity model can give reliable results for heavy components, thus supporting the idea that the larger deviations in the mixtures containing $n$-heptane arise from their asymmetry.

The largest deviations were found for the lowest temperatures, but considering, as presented on Figs. 6–10, that at these temperatures the PR EOS also shows the largest deviations for the liquid densities, it is expected that the viscosity deviations might result from incorrect values from the equation of state.

## 5. CONCLUSIONS

New experimental measurements of viscosity and liquid density of four binary and one ternary $n$-alkane mixtures are presented, increasing the available experimental database for asymmetric systems. Comparison with

pure component data showed that our equipment is able to reproduce literature data with a good accuracy.

The ternary mixture, $n$-$C_7H_{16} + n$-$C_{20}H_{42} + n$-$C_{24}H_{50}$, was compared with the analogous binary, $n$-$C_7H_{16} + n$-$C_{22}H_{46}$. Results showed that although the corresponding liquid densities are quite similar, the viscosity of the binary mixture tends to be higher.

The friction theory, a general and recently proposed model for viscosity, that has already shown to be able to model several fluid mixtures over a broad temperature and pressure range, was used to describe the measured data. In combination with the Peng–Robinson equation of state, and after fitting the critical properties of the heavy alkanes to improve the description of the liquid densities, a good fit of the experimental data was achieved.

## ACKNOWLEDGMENT

A. J. Queimada thanks *Fundação para a Ciência e a Tecnologia* for his Ph.D. scholarship BD/954/2000.

## REFERENCES

1. S. E. Quiñones-Cisneros, C. K. Zéberg-Mikkelsen, and E. H. Stenby, *Fluid Phase Equilib.* **169**:249 (2000).
2. S. E. Quiñones-Cisneros, C. K. Zéberg-Mikkelsen, and E. H. Stenby, *Fluid Phase Equilib.* **178**:1 (2001).
3. S. E. Quiñones-Cisneros, C. K. Zéberg-Mikkelsen, and E. H. Stenby, *Chem. Eng. Sci.* **56**:7007 (2001).
4. C. K. Zéberg-Mikkelsen, S. E. Quiñones-Cisneros, and E. H. Stenby, *Ind. Eng. Chem. Res.* **40**:3848 (2001).
5. C. K. Zéberg-Mikkelsen, S. E. Quiñones-Cisneros, and E. H. Stenby, *Pet. Sci. Technol.* **20**:27 (2002).
6. T. H. Chung, M. Ajlan, L. L. Lee, and K. E. Starling, *Ind. Eng. Chem. Res.* **27**:671 (1988).
7. D. Y. Peng and D. B. Robinson, *Ind. Eng. Chem. Fund.* **15**:59 (1974).
8. Design Institute for Physical Property Data, *DIPPR Database* (AIChE, New York, 1998).
9. A. K. Doolittle and R. H. Peterson, *J. Am. Chem. Soc.* **73**:2145 (1951).
10. S. Dutour, B. Lagourette, and J. Daridon, *J. Chem. Thermodyn.* **33**:765 (2001).
11. E. Giller and H. Drickamer, *Ind. Eng. Chem.* **41**:2067 (1949).
12. B. Knapstad, P. Skjølsvik, and H. Øye, *J. Chem. Eng. Data* **34**:37 (1989).
13. D. Ducoulombier, H. Zhou, C. Boned, J. Peyrelasse, H. Saint-Guirons, and P. Xans, *J. Phys. Chem.* **90**:1692 (1986).
14. N. B. Vargaftik, *Tables on the Thermophysical Properties of Liquids and Gases—in Normal and Dissociated States*, 2nd Ed. (Wiley, New York, 1975).
15. M. J. Assael, C. P. Oliveira, M. Papadaki, and W. A. Wakeham, *Int. J. Thermophys.* **13**:593 (1992).
16. T. M. Aminabhavi, V. B. Patil, M. I. Aralaguppi, and H. T. S. Phayde, *J. Chem. Eng. Data* **41**:521 (1996).
17. M. I. Aralaguppi, C. V. Jadar, and T. M. Aminabhavi, *J. Chem. Eng. Data* **44**:435 (1999).

18. D. S. Viswanath and G. Natarajan, *Data Book on the Viscosity of Liquids* (Hemisphere, New York, 1989).
19. D. L. Wakefield, K. N. Marsh, and B. J. Zwolinski, *Int. J. Thermophys.* **9**:47 (1988).
20. A. Y. Dandekar, S. I. Andersen, and E. H. Stenby, *J. Chem. Eng. Data* **43**:551 (1998).
21. A. J. Queimada, E. H. Stenby, I. M. Marrucho, and J. A. P. Coutinho, *Fluid Phase Equilib.* **212**:303 (2003).